Geophysical Research Letters

RESEARCH LETTER
10.1029/2020GL092126

Satellite Remote Sensing of Herring (*Clupea pallasii*) Spawning Events: A Case Study in the Strait of Georgia

Lin Qi[1,2,3], Shuai Zhang[3], Alexander J. Manos[3], Douglas E. Hay[4], Bruce McCarter[4], Menghua Wang[5], Karlis Mikelsons[5,6], and Chuanmin Hu[3]

[1]School of Marine Sciences, Sun Yat-Sen University (SYSU), Guangzhou, China, [2]Southern Marine Science and Engineering Guangdong Laboratory (Zhuhai), Zhuhai, China, [3]College of Marine Science, University of South Florida, St. Petersburg, FL, USA, [4]Pacific Biological Station, Fisheries and Oceans Canada, Nanaimo, BC, Canada, [5]Center for Satellite Applications and Research, National Oceanic and Atmospheric Administration, College Park, MD, USA, [6]Global Science and Technology, Inc., Greenbelt, MD, USA

Key Points:

- Satellite remote sensing is shown to be able to detect herring spawning events in certain regions
- Coastal waters rich in herring milt show unique reflectance shapes that can be distinguished from other bright features
- Multi-sensor images reveal spatial and temporal characteristics of herring spawning events in the Strait of Georgia

Supporting Information:

Supporting Information may be found in the online version of this article.

Correspondence to:

C. Hu,
huc@usf.edu

Citation:

Qi, L., Zhang, S., Manos, A. J., Hay, D. E., McCarter, B., Wang, M., et al. (2021). Satellite remote sensing of herring (*Clupea pallasii*) spawning events: A case study in the Strait of Georgia. *Geophysical Research Letters*, *48*, e2020GL092126. https://doi.org/10.1029/2020GL092126

Received 17 DEC 2020
Accepted 9 MAR 2021

Abstract In this proof-of-concept study, we show how satellite remote sensing can be used to detect and monitor Pacific herring spawning events in the Strait of Georgia (SoG), British Columbia, Canada. Multi-sensor medium-resolution (~300 m) and high-resolution (3–30 m) images reveal bright waters in the SoG due to high concentrations of herring milt from multiple spawning events. The milt-infused waters lead to enhanced reflectance with unique spectral characteristic that can be distinguished from other optically active constituents such as suspended sediments, coccolithophores, "whiting" particles, and shallow bottoms. While the medium-resolution images may be used to search for cloud-free and potential spawning sites, high-resolution images show more details in milt distributions. Given the increased availability of high-resolution satellite imagery at the global scale, this demonstration may promote more applications of satellite remote sensing in fisheries and ocean ecology research.

Plain Language Summary This proof-of-concept study demonstrates that certain fish spawning events can produce a bright enough signal in satellite images that may allow satellite-based observations to assist with some aspects of fisheries management. Specifically, herring spawning events in the Strait of Georgia (British Columbia, Canada, and the Gulf of Alaska) can be observed in images collected by various satellite sensors, and the spatial extent of some spawning events can also be characterized and quantified. This is because the reflectance shape of waters rich in herring milt is unique and allows herring spawn to be distinguished without ambiguity relative to other waters. The ability to detect these spawning events has major implications for satellite remote sensing, which can provide complementary information to data collected from expensive and weather-dependent in situ SCUBA and shipboard surveys. Further, satellite observations could be used to test the completeness and geographical precision and accuracy of other surveys, especially airborne surveys, for example through characterizing herring spawning events at synoptic scales.

1. Introduction

Traditional methods for directly evaluating fisheries have included bottom trawl surveys (Link et al., 2002), genetic studies (Carvalho & Hauser, 1995), acoustic surveys (Bailey et al., 1998), and airborne surveys (Churnside et al., 2017), with the latter being the primary non-shipboard remote sensing means to directly assess populations of fish and other animals (e.g., herring schools around the Georges Bank in the North Atlantic, Borstad et al., 1992). In contrast, satellite remote sensing has been used to collect environmental data (e.g., sea surface temperature, chlorophyll-*a* concentration) to give a holistic view of the environment (Chassot et al., 2011; Klemas, 2013; McCarthy et al., 2017; Santos, 2000; Stuart et al., 2011), as direct observations of fish populations is difficult due to the small size and ephemeral nature of fish schools relative to the spatial resolution and temporal coverage of available satellite imagery.

However, a specific question is whether it is possible to detect fish spawning events, as aggregation of fish milt or eggs in surface waters may result in a signal large enough and long enough (e.g., hours to days) that can be captured by satellite imagery. Recent advances in satellite remote sensing of spawning by some salt-water animals suggest that this question is worth exploring. For example, a coral spawning event near

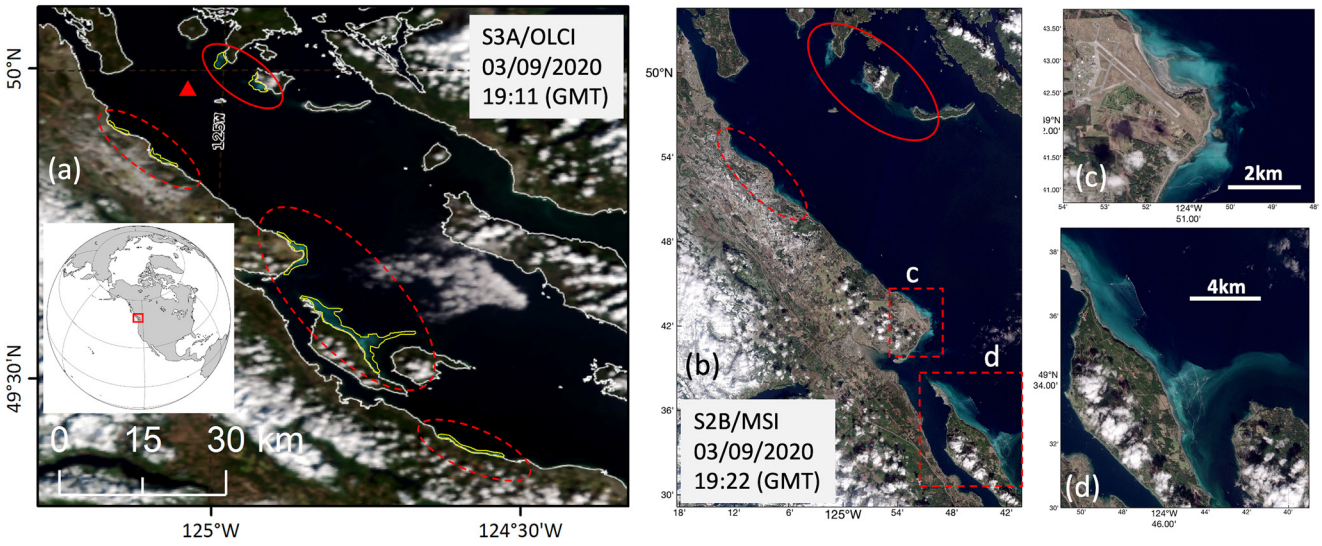

Figure 1. (a) Ocean and Land Colour Instrument (OLCI) image on March 9, 2020 showing several herring spawning areas (yellow polygons, with red ellipses indicating the locations) in the Strait of Georgia (SoG) near Vancouver Island. The red triangle shows the location of buoy #46131. (b) Multi Spectral Instrument (MSI) image on the same day. The red boxes highlight two herring spawning sites, with more details shown in (c) and (d), respectively. The solid red ellipse lines in (a) and (b) show two herring spawning sites not captured in satellite images before 2020.

Japan has been captured by satellite imagery due to the distinguishable reflectance of the coral eggs (Yamano et al., 2020), and images slicks captured over the Great Salt Lake (USA) appear to be a result of surface aggregation of brine shrimp cysts (Qi et al., 2020). An online search of fish spawn resulted in digital photos of herring spawning events, where high concentrations of herring milt make the water appear brighter than the surrounding environment. Various studies and online documents have also reported the use of field crews, SCUBA divers, and airborne surveys to document herring spawn distributions, habitat size, and long-term changes (Hay & McCarter, 2015; Hay et al., 2009; Hebert, 2020; Hulson et al., 2008). Yet the same literature search showed no study on satellite remote sensing of herring spawn, possibly due to the ephemeral nature of herring spawning events and coarse resolution of most satellite images. On the other hand, once proven effective, satellite remote sensing may provide complementary information on these spawning events, which can be useful for fisheries models to describe the recruitment and abundance of juvenile and adult members of the population and the influence they may have on other species (Boldt et al., 2019; Fox et al., 2018).

The increased availability of multi-sensor and multi-resolution satellite imagery raises the following question: to what extent can ephemeral and small-scale events, such as herring spawning, be captured by the various satellite sensors? The objective of this study is to develop and demonstrate a practical approach to search, detect, and quantify herring spawning events through the use of various publicly available optical sensor data.

2. Data and Methods

2.1. Study Region

The study selected the Strait of Georgia (SoG, Figure 1a) in British Columbia, Canada, because: (1) herring spawning events have been reported here (Haegele & Schweigert, 1985; Hay & McCarter, 2015) and (2) the region is important both ecologically and economically (Haegele & Schweigert, 1985; Hay et al., 2001; Trochta et al., 2020). As planktivores, herring provide a direct link between primary producers and animals of higher trophic levels including Chinook salmon (Boldt et al., 2019; Fox et al., 2018; Varpe et al., 2005). During the spawning season, adult herring migrate from deeper oceanic waters to shallow, intertidal and subtidal zones to release their milt in the water and deposit their eggs on macrophyte substrates such as seagrass and seaweeds (Haegele et al., 1982).

2.2. Data Sources

Two online tools were used to complement each other in their spatial and temporal coverage/resolutions. The first is the OCView tool, developed by the NOAA STAR Ocean Color Research Team (Mikelsons & Wang, 2018), which was utilized to browse the Visible Infrared Imaging Radiometer Suite (VIIRS) images and Sentinel-3 Ocean and Land Colour Instrument (OLCI) images at ~300 m resolution for cloud free conditions and for possible spawning events. The second tool is the Sentinel Hub EO Browser, which allows a user to browse quick-look images in more details using the Sentinel-2 Multi Spectral Instrument (MSI) data (10–20 m spatial resolution).

For more in-depth analysis, MSI and OLCI data were downloaded from the European Space Agency's Sentinel open access hub (https://scihub.copernicus.eu/dhus/#/home), and then processed using the Acolite and SeaDAS software (version 7.5) to generate spectral Rayleigh corrected reflectance (R_{rc}, dimensionless) and remote sensing reflectance (R_{rs}, sr^{-1}), respectively.

Planet Scope/DOVE 3-m resolution data were downloaded from the Planet Lab, Inc. (http://www.planet.com). These high-resolution data in four spectral bands were collected by optical sensors from a constellation of hundreds of miniature satellites (CubeSats). They were used to estimate cloud-free data availability and to characterize the observed herring spawning features. The Moderate Resolution Imaging Spectroradiometer (MODIS) data (2000–2020) were downloaded from the NASA GSFC (https://oceancolor.gsfc.nasa.gov), and then processed using SeaDAS to generate spectral R_{rc} data at 250-m resolution, from which true-color images were generated and inspected. Likewise, Landsat data were downloaded from the Google Earth Engine, and processed and inspected in a similar fashion.

Wind and sea surface temperature (SST) data were obtained from the Environment and Climate Change Canada Sentry Shoal buoy (# 46131, red triangle in Figure 1a) accessed via the NOAA National Data Buoy Center (NDBC, https://www.ndbc.noaa.gov/).

2.3. Methods

The OCView and EO Browser tools were used to first determine the approximate locations and timings of conspicuously bright features as possible herring spawning events within the SoG around the peak spawning season. The corresponding high-resolution MSI and DOVE data were inspected to obtain more details, and the corresponding OLCI and MSI data were processed to perform the spectral analysis. R_{rs} spectra (412–709 nm) of the spawning waters in the SoG were compared with those from another spawning event near Kayak Island (off the coast of southern Alaska in the Gulf of Alaska [GoA]), and compared with those extracted from other bright targets in the SoG and in other coastal waters. The similarity between two spectra was estimated through a spectral angle measure (SAM), calculated using Equation 1 (Kruse et al., 1993).

$$\theta = \cos^{-1}\frac{\sum x \cdot y}{\sqrt{\sum x^2 \sum y^2}} \tag{1}$$

where x is a vector of the reference (herring spawn in the SoG) spectra and y is a vector of the target spectra to be evaluated. An angle of 0° indicates two identical spectra shapes. By definition, SAM only measures the spectral shape as opposed to magnitude. In this regard, if plotted in logarithmic scale, SAM = 0° indicates two spectra parallel to each other even if their magnitudes can differ by 10 times. For this reason, it is possible that when only several bands become near-parallel, these bands may be selected to calculate the SAM in order to distinguish the various types of bright targets.

3. Results

3.1. Image Inspection

The use of the OCView and EO Browser online tools allowed for a quick inspection of VIIRS, OLCI, and MSI images, which often showed bright patches along the coasts of Vancouver Island and other smaller islands. Figure 1a shows an OLCI example on March 9, 2020, while the entire image archive showed similar events in 2020 and other years, all in March (see Figure S1). The corresponding MSI images show similar

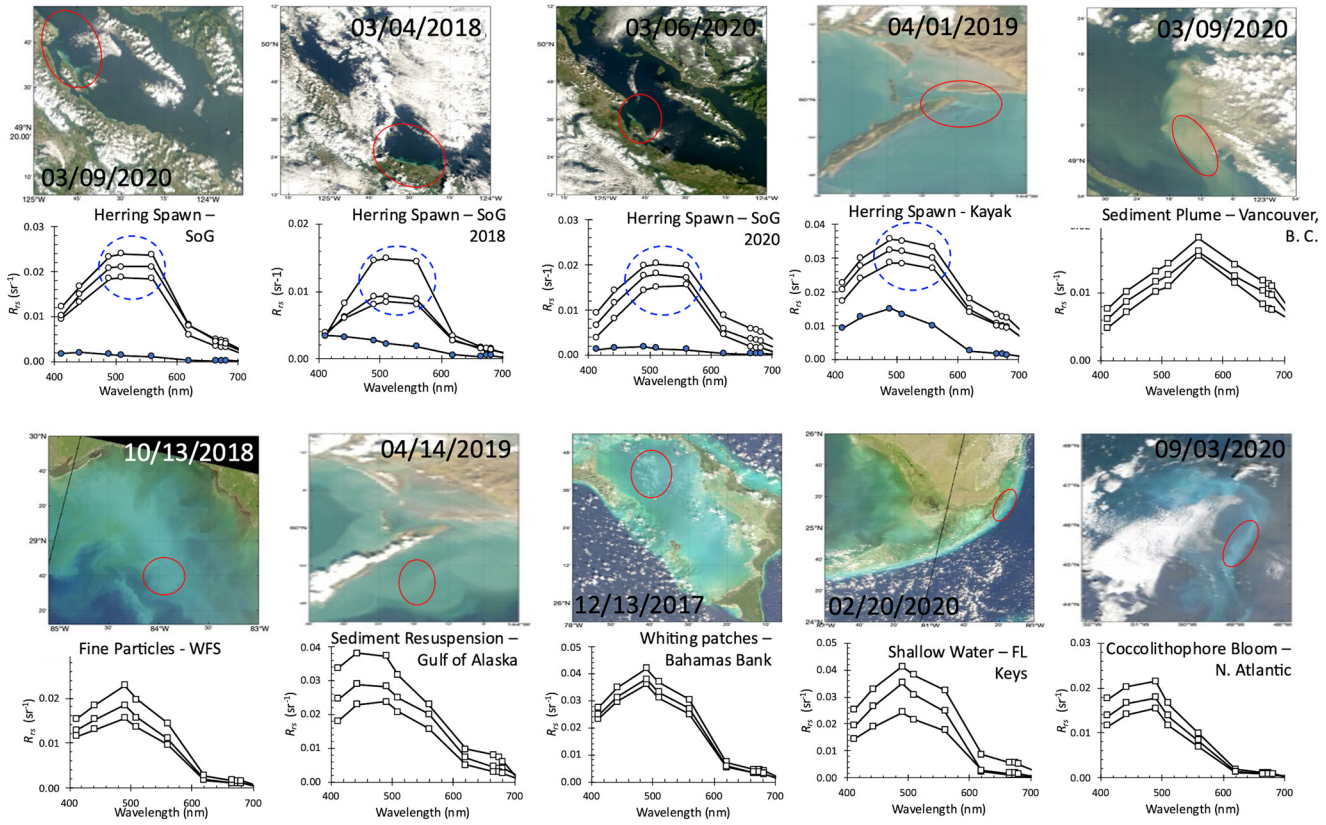

Figure 2. Ocean and Land Colour Instrument (OLCI) true-color RGB images of various bright targets and their associated spectra (open circles). First and second rows left to right: herring spawn from the Strait of Georgia (SoG) (3 panels), herring spawn near Kayak island of the Gulf of Alaska (GoA), and terrigenous sediment plume (Fraser River near Vancouver, British Columbia, Canada); Third and fourth rows left to right: post-hurricane sediment resuspension on the west Florida shelf (WFS), sediment resuspension in the GoA, $CaCO_3$ whiting event in Bahamas Bank (Lloyd, 2012), optically shallow water in the Florida Keys (USA) (Barnes et al., 2018), and coccolithophore bloom in the North Atlantic Ocean (Moore et al., 2012). The filled circles in the second row represent the R_{rs} spectra of waters adjacent to the herring spawning waters. The three bands that are used to differentiate spawning waters from other bright targets are circled in blue.

bright patches but in greater detail at 10-m resolution (Figures 1b–1d), where more high-resolution images can be found in Figure S2. These bright, turquoise-colored waters are clearly distinct from the surrounding environment (Figures 1b–1d and 2, Figure S3). They also agree with the documented herring spawning records both in time and location (https://maps.sogdatacentre.ca/app/dashboard-map-of-herring-spawn-in-the-strait-of-georgia-1951-to-2019), and therefore can be confirmed as herring spawning events.

3.2. Spectral Characterization

The bright water patches are apparently due to enhanced reflectance of high concentration of fish milt, as images collected in February or late March did not show similar bright patches even under strong winds (>8 m s^{-1}). The pixels in the bright patches all show elevated reflectance in all wavelengths as compared with nearby waters, further confirming that the enhanced reflectance is caused by highly scattering particles rather than by phytoplankton or colored dissolved organic matter because they both strongly absorb light in the blue wavelengths. The question of interest is whether such enhanced reflectance can be distinguished from other bright targets caused by either high concentrations of non-milt particles or shallow bottom features in the SoG and also in other coastal waters. Such knowledge may help identify milt-rich waters when searching for potential spawning spots in the SoG and elsewhere. Figure 2 shows the representative images of these bright targets together with their R_{rs} spectra. Visually, all these bright targets appear similar, and they all show higher reflectance between 443 and 560 nm than in other wavelengths. Indeed, when all wavelengths are used in calculating the SAM (Equation 1) between these targets and SoG

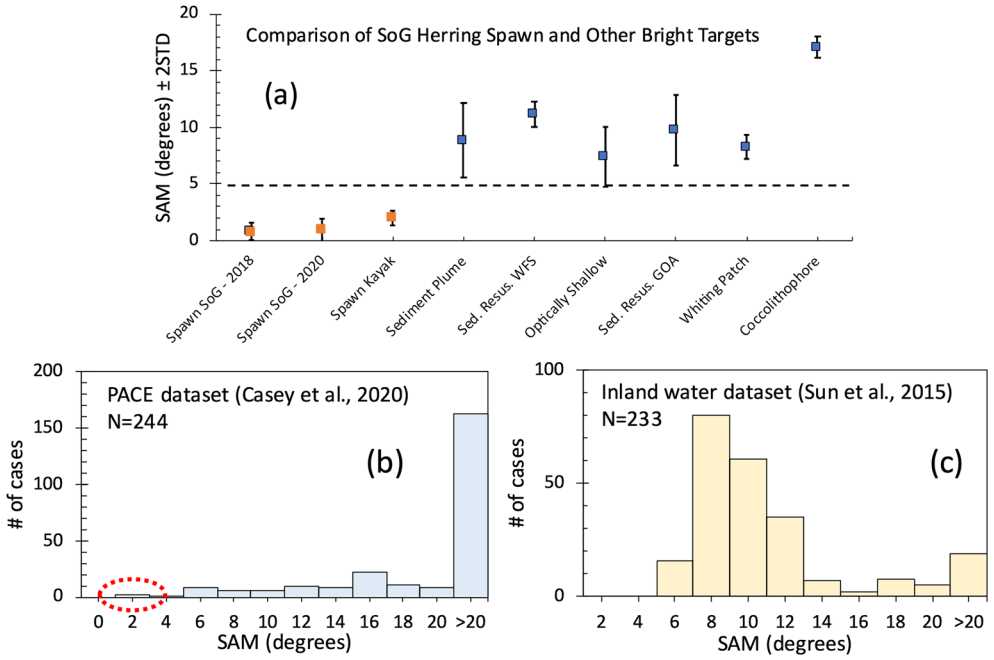

Figure 3. (a) The spectral angle measure (SAM, degrees) between the herring spawn spectra from the SoG on March 9, 2020 and other herring spawn spectra from the Strait of Georgia (SoG) and Kayak Island as well as from other bright targets (Figure 2). SAM was calculated using Equation 1 and three OLCI bands (490, 510, 560 nm). The dashed line marks 5°. Vertical bars indicate two standard deviations (STDs). (b) and (c): SAM between R_{rs}(490–560 nm) from SoG herring spawning waters and from global waters (b) and inland waters (c), respectively. In (b), the original data set of 949 R_{rs} spectra was screened to exclude dark waters (R_{rs}(490–560) <0.005 sr^{-1}) as these waters cannot be herring spawning waters. The only two cases with SAM <5° (red ellipse in (b)) occurred in nearshore waters around Shell Island, NE Gulf of Mexico (30.118 N & 85.734 W, 30.113 N & 85.736 W) that cannot be herring spawning waters. Similar results from MSI data are shown in Figure S3.

herring spawn bright pixels, it is not always possible to differentiate them as their SAM values are similar (i.e., <10°, sometimes approaching 5°). However, when only three wavelengths are used (490, 510, 560 nm, blue circles in Figure 2), the SAM values from herring spawn bright pixels are statistically different from all other bright targets (Figure 3a), suggesting that these unique spectral shapes between 490 and 560 nm can be used to identify herring spawning events, at least for this study region. Tests over the same types of bright targets from other images showed the same results. Furthermore, when testing over a compiled R_{rs} data set for global waters (Casey et al., 2020) and for inland waters (Sun et al., 2015), there is nearly no exception that all these waters have their SAM values >5° if referenced against the herring spawn R_{rs} spectra (Figures 3b and 3c), further proving the unique spectral shape between 490 and 560 nm from herring spawning waters. The same test using MSI bands of 490 and 560 nm also confirmed this observation (Figure S3), as non-spawn bright pixels from shallow waters, inter-tidal zone, and suspended sediments in the SoG all showed different spectral shapes (relatively large SAM values) from herring spawn pixels.

It is interesting to see that while not all these bright targets (including herring spawn) are statistically different when R_{rs} at all spectral bands are used to calculate the SAM, the use of just R_{rs} at three bands leads to different results. A close inspection of all R_{rs} spectra in Figure 2 suggests that this does make sense. Between the two spawning events in the SoG and near Kayak Island, their reflectance are rather flat and nearly horizontal between 490 and 560 nm (blue circles in Figure 2). This characteristic appears unique, as all other bright targets show apparent reflectance peak at either 490, 510, or 560 nm. The SAM is therefore a reliable measure of such characteristics using R_{rs} at the three bands. In contrast, if R_{rs} at all spectral bands are used to calculate the SAM, because all bright targets show the same spectral shapes of low-high-low at the blue-green-red bands, their SAM values are not always different statistically. In other words, adding R_{rs} at more blue or red bands will "smear" the spectral contrast between herring spawn waters and other bright targets.

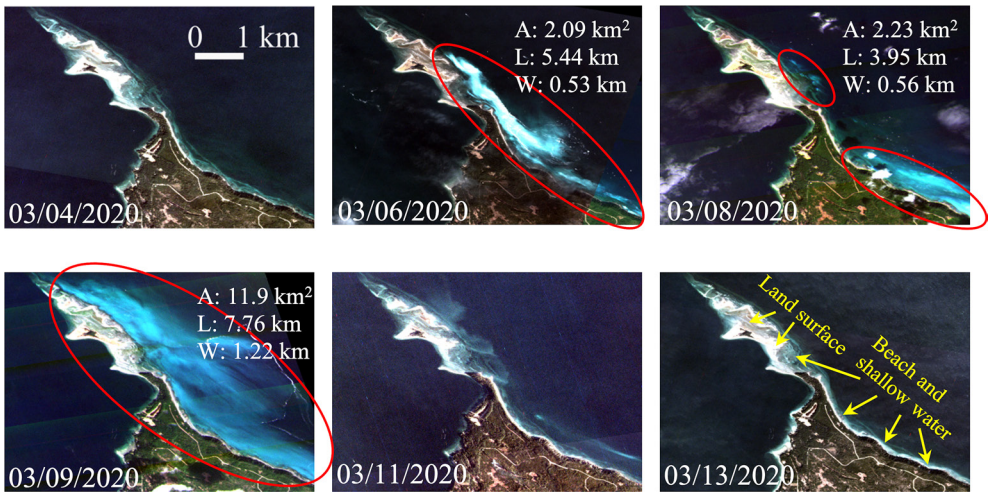

Figure 4. Cloud-free DOVE image sequence for one spawning site in the SoG during the spawning season of March 1–15, 2020. The bright herring spawn waters are within the red ellipses. The whitish and dark blue-greenish colors in the images represent land surface, beaches, and shallow waters that are spectrally different from herring spawn waters (Figures 2 and 3). The milt-rich spawn waters are characterized by their area (A), length (L), and width (W).

3.3. Spatial Characterization

Because the synoptic measurements of the study region occur within seconds, satellite images can reveal spatial characteristics of herring spawn waters in different sites almost simultaneously, making it possible to characterize each spawning site at the same time. Corresponding to the MSI image in Figure 1b, the precise coastal locations of milt-rich discolored waters correspond to locations of the documented records where herring eggs occur and are shown as multiple one-km coastal segments estimated from annual SCUBA diver surveys (Hay & McCarter, 2015) (https://www.pac.dfo-mpo.gc.ca/science/species-especes/pelagic-pelagique/herring-hareng/herspawn/142fig-eng.html). Herring eggs are adhesive and are deposited mainly in the inter-tidal and shallow sub-tidal areas (usually less than 20 m depth) (Haegele et al., 1982). SCUBA diver surveys examine egg distributions whereas satellite images reveal milt distributions, which are more ephemeral because milt may disperse rapidly depending on local tidal and weather activity. For instance, from satellite observations shown in Figure 1b, the total area of milt-rich water in the SoG locations was estimated to be ~42 km^2, with an average width of 860 ± 520 m. In contrast, the mean width of egg depositions is lower, and usually between 100 and 200 m. Therefore, depths of documented egg depositions and depths of water where milt discoloration occurs may not necessarily be identical.

The high-resolution images also allowed characterization of spawning waters in each site and how they changed over time. Figure 4 shows a sequence of cloud-free DOVE images (3-m resolution) over one spawning site in the SoG, where the area, length, and width of the milt-rich spawning waters are annotated in each image. More examples of DOVE are shown to illustrate the daily changes (Figure S4) and diel changes (Figure S5). It is clear that these high-resolution, repeated cloud-free images can be used to characterize herring spawning events rapidly and in a cost-effective way.

4. Discussion

In the past several decades, a mix of diver surveys, airborne visual observations, digital photo, video, and photographic imaging have been used operationally for herring in British Columbia and Alaska and capelin in Newfoundland (Nakashima, 1992). Long-term maps of Spawn Habitat Index (SHI) for herring of the SoG have been generated through mainly diver surveys (Hay & McCarter, 2015; Hebert, 2020). Visual and photographic aerial surveys have also been used elsewhere for sardines, whales, sharks, rays, turtles, tuna, marine birds, and other marine mammals. However, remote sensing of either fish, fish milt, or fish eggs using satellites has not been possible due to the small size of fish schools (relative to the size of a satellite

image pixel) and the ephemeral nature of fish aggregation or fish spawning. In this regard, the study here may represent a novel application of satellite remote sensing in fisheries studies.

There are probably no other phenomena that could be mistakenly confused with herring spawns captured by satellite imagery. Few, if any other fish or invertebrate species spawning inter-tidally or in shallow, sub-tidal locations could change water color in any way that might be mistaken for herring. Potential exceptions might include the spawning of oysters, or other bivalves, where the nearshore water clarity and color might be altered but such events usually are relatively small, less conspicuous and occur at different times of the year and in locations and habitats not normally used for herring spawning.

Given the past and ongoing operational effort to characterize herring spawning in the SoG and the GoA, the pertinent question is what additional value can satellite observations bring to the table. As shown in the examples above, one advantage is in their freely available data combined with their synoptic and frequent coverage. This capability could be especially important as a potential tool to document spawning in remote or inaccessible locations where SCUBA and aerial surveys cannot occur. Also, as indicated by the results from the spectral analysis above, the ability to differentiate between herring milt deposition and other sources of water discoloration could have potential for addressing many instances of coastal management as well as providing input to herring assessment and management. The herring spawning features captured in satellite imagery may thus provide complementary information to those available using other means, for example through estimating the length of the herring spawning waters in different locations of the SoG simultaneously. Once multiple images are available in the same spawning season, it may also be possible to evaluate the short-term changes of herring spawning (e.g., Figure 4). Such characteristics can be difficult to obtain through diver observations, in situ acoustic surveys, or airborne observations as they are time and resource intensive (Klemas, 2013; Santos, 2000). Finally, as satellite images are collected in a near real-time fashion with no *a priori* knowledge required to target an area, new "hotspots" of herring spawn may be captured.

The findings also have implications in a broader context than just the SoG. The spectral characteristics of herring spawn waters (Figures 2 and 3, Figure S3) make it possible to develop an approach to search for herring spawning sites in other regions (Haegele & Schweigert, 1985; Watters et al., 2004) before a targeted study may be initiated. Specifically, suspicious and ephemeral bright features may be recorded through image inspections using the OCView and the EO Browser tools. Spectral shapes from these features derived from OLCI and/or MSI, or historical reports of herring spawning, may confirm whether these suspicious features are due to herring spawning or other causes. Subsequent analysis of high-resolution satellite data can then be used to characterize the herring spawning events.

It appears that all optical sensors are capable of detecting herring spawning events in the SoG as long as their spatial resolutions are sufficient to capture these small-scale bright targets and satellite data are collected under cloud-free conditions. One potential drawback is the scarce availability of high-resolution data, especially when cloud cover is considered. However, a combination of two MSI sensors on Sentinel-2A and Sentinel-2B, respectively, may revisit a site every 2–3 days. The DOVE constellation, on the other hand, may provide daily revisits during the spawning season even after discounting cloud cover (Figures S5 and S6), and the revisit frequency appears to increase continuously due to increased number of satellites (Figure S6). Future satellite missions may even make it possible to "stare" at a given site multiple times a day, for example through geostationary satellite platforms. One may speculate that high winds may lead to sediment resuspension and/or high waves that make it difficult to observe herring spawning events. Yet statistics of winds indicate that this is not the case, as these events can be observed even under strong winds of 13 m s^{-1} (Figure S7). Therefore, given the availability of satellite data to all researchers global wide, the demonstration here may promote future satellite applications in fisheries studies.

Despite the advantage shown here in satellite remote sensing of herring spawning events, this study is still preliminary. For example, although each detected spawning site can be characterized for its area, length, and width of the milt-rich waters, it is unclear whether concentrations of herring milt can be quantified. This challenge may be addressed in the future through targeted and coordinated field surveys to quantify the relationships between milt concentration and reflectance, from which an optical model may be developed and applied to satellite remote sensing. In this way, not only can the size of the detected spawning site

be quantified, but the spawning strength of each site may also be estimated, thus providing complementary information to the existing SHI calculated using surface and diver survey data.

5. Conclusions

This proof-of-concept study represents the first attempt to use publicly available satellite remote sensing data to characterize fish spawning events, specifically herring spawning in the SoG, British Columbia, Canada. The combined use of the NOAA OCView and the EO Browser online tools as well as multi-sensor data from OLCI, MSI, and DOVE suggest that, under cloud-free conditions, herring spawning can be detected and differentiated from other events. Further imagery of herring spawning in each detected site may provide some approximate estimation of the magnitude of spawning, especially through the estimation of the cumulative linear distance of coastline where milt occurs. While preliminary in nature, the study is expected to stimulate more satellite remote sensing applications in fisheries studies.

Data Availability Statement

Most satellite data used in this study are public domain, available from NASA (MODIS, https://oceancolor.gsfc.nasa.gov), NOAA VIIRS, https://www.star.nesdis.noaa.gov/socd/mecb/color/ocview/ocview.html), and ESA (OLCI and MSI, https://scihub.copernicus.eu/dhus/#/home). PlanetScope/DOVE were provided by Planet Lab, Inc. through the Commercial Archive Data for NASA investigators (cad4nasa.gsfc.nasa.gov) under the National Geospatial-Intelligence Agency's NextView license agreement.

Acknowledgments
This study was supported by the National Natural Science Foundation of China (No. 41806208; No. 42076180), the U.S. NOAA (NA15OAR4320064), and the U.S. NASA (80NSSC21K0422, 80NSSC20M0264). The scientific results and conclusions, as well as any views or opinions expressed herein, are those of the authors and do not necessarily reflect those of NOAA or the Department of Commerce. The authors thank the two anonymous reviewers for providing insightful comments and suggestions.

References

Bailey, M., Maravelias, C. D., & Simmonds, E. J. (1998). Changes in the spatial distribution of autumn spawning herring (Clupea harengus L.) derived from annual acoustic surveys during the period 1984-1996. *ICES Journal of Marine Science*, *55*, 545–555. https://doi.org/10.1006/jmsc.1998.0355

Barnes, B. B., Garcia, R., Hu, C., & Lee, Z. (2018). Multi-band spectral matching inversion algorithm to derive water column properties in optically shallow waters: An optimization of parameterization. *Remote Sensing of Environment*, *204*, 424–438. https://doi.org/10.1016/j.rse.2017.10.013

Boldt, J., Thompson, M., Rooper, C., Hay, D., Schweigert, J., Quinn TJ, I., et al. (2019). Bottom-up and top-down control of small pelagic forage fish: Factors affecting age-0 herring in the Strait of Georgia, British Columbia. *Marine Ecology Progress Series*, *617*, 53–66. https://doi.org/10.3354/meps12485

Borstad, G. A., Hill, D. A., Kerr, R. C., & Nakashima, B. S. (1992). Direct digital remote sensing of herring schools. *International Journal of Remote Sensing*, *13*(12), 2191–2198. https://doi.org/10.1080/01431169208904262

Carvalho, G. R., & Hauser, L. (1995). Molecular genetics and the stock concept in fisheries. *Reviews in Fish Biology and Fisheries*, *4*, 326–350

Casey, K. A., Rousseaux, C. S., Gregg, W. W., Boss, E., Chase, A. P., Craig, S. E., et al. (2020). A global compilation of in situ aquatic high spectral resolution inherent and apparent optical property data for remote sensing applications. *Earth System Science Data*, *12*, 1123–1139. https://doi.org/10.5194/essd-12-1123-2020

Chassot, E., Bonhommeau, S., Reygondeau, G., Nieto, K., Polovina, J. J., Huret, M., et al. (2011). Satellite remote sensing for an ecosystem approach to fisheries management. *ICES Journal of Marine Science*, *68*(4), 651–666. https://doi.org/10.1093/icesjms/fsq195

Churnside, J., Wells, R. D., Boswell, K., Quinlan, J., Marchbanks, R., McCarty, B., & Sutton, T. (2017). Surveying the distribution and abundance of flying fishes and other epipelagics in the northern Gulf of Mexico using airborne lidar. *Bulletin of Marine Science*, *93*, 591–609. https://doi.org/10.5343/bms.2016.1039

Fox, C., Paquet, P., & Reimchen, T. (2018). Pacific herring spawn events influence nearshore subtidal and intertidal species. *Marine Ecology Progress Series*, *595*, 157–169. https://doi.org/10.3354/meps12539

Haegele, C. W., Humphreys, R. D., & Hourston, A. S. (1982). Distribution of eggs by depth and vegetation type in Pacific herring (*Clupea harengus pallasi*) spawnings in southern British Columbia. *Canadian Journal of Fisheries and Aquatic Sciences*, *38*(4), 381–386

Haegele, C. W., & Schweigert, J. F. (1985). Distribution and characteristics of herring spawning grounds and description of spawning behavior. *Canadian Journal of Fisheries and Aquatic Sciences*, *42*, 39–55. https://doi.org/10.1139/f85-261

Hay, D. E., & McCarter, P. B. (2015). Revised from Hay, D.E., & P.B. McCarter R. Kronlund and C. Roy. (1989). *Spawning areas of British Columbia herring: A review, geographical analysis and classification* (Canadian Data Report of Fisheries and Aquatic Science 2019, Vol. 1–6). Retrieved from https://www.pac.dfo-mpo.gc.ca/science/species-especes/pelagic-pelagique/herring-hareng/herspawn/pages/project-eng.html

Hay, D. E., McCarter, P. B., Daniel, K. S., & Schweigert, J. F. (2009). Spatial diversity of Pacific herring (*Clupea pallasi*) spawning areas. *ICES Journal of Marine Science*, *66*, 1662–1666. https://doi.org/10.1093/icesjms/fsp139

Hay, D. E., Toresen, R., Stephenson, R., Thompson, M., Claytor, R., Funk, F., et al. (2001). Taking stock: An inventory and review of world herring stocks in 2000. In F. Funk, J. Blackburn, & D. Hay (Eds.), *Lowell wakefield symposium. Vol. Herring: Expectations for a new millennium* (pp. 381–454). Anchorage, AK. University of Alaska Sea Grant College Program.

Hebert, K. (2020). *Southeast Alaska 2019 herring stock assessment surveys* (Fishery Data Series No. 20-23). Anchorage, AK. Alaska Department of Fish and Game. Retrieved from https://www.adfg.alaska.gov/FedAidPDFs/FDS20-23.pdf

Hulson, P.-J. F., Miller, S. E., Quinn, T. J., Marty, G. D., Moffitt, S. D., & Funk, F. (2008). Data conflicts in fishery models: Incorporating hydroacoustic data into the Prince William Sound Pacific herring assessment model. *ICES Journal of Marine Science*, *65*, 25–43. https://doi.org/10.1093/icesjms/fsm162

Klemas, V. (2013). Fisheries applications of remote sensing: An overview. *Fisheries Research*, *148*, 124–136. https://doi.org/10.1016/j.fishres.2012.02.027

Kruse, F. A., Lefkoff, A. B., Boardman, J. W., Heidebrecht, K. B., Shapiro, A. T., Barloon, P. J., & Goetz, A. F. H. (1993). The spectral image processing system (SIPS)-interactive visualization and analysis of imaging spectrometer data. *Remote Sensing of Environment*, *44*, 145–163. https://doi.org/10.1016/0034-4257(93)90013-n

Link, J. S., Brodziak, J. K. T., Edwards, S. F., Overholtz, W. J., Mountain, D., Jossi, J. W., et al. (2002). Marine ecosystem assessment in a fisheries management context. *Canadian Journal of Fisheries and Aquatic Sciences*, *59*, 1429–1440. https://doi.org/10.1139/f02-115

Lloyd, R. A. (2012). *Remote sensing of whitings in the Bahamas* (Graduate Theses and Dissertations). Retrieved from https://scholarcommons.usf.edu/etd/4361

McCarthy, M. J., Colna, K. E., El-Mezayen, M. M., Laureano-Rosario, A. E., Méndez-Lázaro, P., Otis, D. B., et al. (2017). Satellite remote sensing for coastal management: A review of successful applications. *Environmental Management*, *60*, 323–339. https://doi.org/10.1007/s00267-017-0880-x

Mikelsons, K., & Wang, M. (2018). Interactive online maps make satellite ocean data accessible. *Eos*, *99*. https://doi.org/10.1029/2018eo096563

Moore, T. S., Dowell, M. D., & Franz, B. A. (2012). Detection of coccolithophore blooms in ocean color satellite imagery: A generalized approach for use with multiple sensors. *Remote Sensing of Environment*, *117*, 249–263. https://doi.org/10.1016/j.rse.2011.10.001

Nakashima, B. S. (1992). *Results of aerial surveys of capelin (Mallotus villosus)* schools using the compact airborne spectrographic imager (CASI) (Northwest Atlantic Fisheries Organization Scientific Council Reports, Serial No. N2038). Retrieved from https://www.nafo.int/Portals/0/PDFs/sc/1992/scr-92-005.pdf

Qi, L., Hu, C., Mikelsons, K., Wang, M., Lance, V., Sun, S., et al. (2020). In search of floating algae and other organisms in global oceans and lakes. *Remote Sensing of Environment*, *239*, 111659. https://doi.org/10.1016/j.rse.2020.111659

Santos, A. M. P. (2000). Fisheries oceanography using satellite and airborne remote sensing methods: A review. *Fisheries Research*, *49*, 1–20. https://doi.org/10.1016/s0165-7836(00)00201-0

Stuart, V., Platt, T., & Sathyendranath, S. (2011). The future of fisheries science in management: A remote-sensing perspective. *ICES Journal of Marine Science*, *68*(4), 644–650. https://doi.org/10.1093/icesjms/fsq200

Sun, D., Hu, C., Qiu, Z., & Wang, S. (2015). Reconstruction of hyperspectral reflectance for optically complex turbid inland lakes: Test of a new scheme and implications for inversion algorithms. *Optics Express*, *23*, A718–A740. https://doi.org/10.1364/OE.23.00A718

Trochta, J. T., Branch, T. A., Shelton, A. O., & Hay, D. E. (2020). The highs and lows of herring: A meta-analysis of patterns and factors in herring collapse and recovery. *Fish and Fisheries*, *21*, 639–662. https://doi.org/10.1111/faf.12452

Varpe, Ø., Fiksen, Ø., & Slotte, A. (2005). Meta-ecosystems and biological energy transport from ocean to coast: The ecological importance of herring migration. *Oecologia*, *146*, 443–451. https://doi.org/10.1007/s00442-005-0219-9

Watters, D. L., Brown, H. M., Griffin, F. J., Larson, E. J., & Cherr, G. N. (2004). Pacific herring spawning ground in San Francisco Bay: 1973-2000. *American Fisheries Society Symposium*, *39*, 3–14

Yamano, H., Sakuma, A., & Harii, S. (2020). Coral-spawn slicks: Reflectance spectra and detection using optical satellite data. *Remote Sensing of Environment*, *251*, 112058. https://doi.org/10.1016/j.rse.2020.112058